PŮVODNÍ PRÁCE/ORIGINAL PAPER

Molecular structure of tangdanite from the Jánská vein, Příbram (Czech Republic) - a vibrational spectroscopy study

Pavel Škácha*, Jiří Sejkora and Jiří Čejka

*Department of Mineralogy and Petrology, National Museum, Cirkusová 1740, 193 00 Praha 9 - Horní Počernice; *e-mail: skachap@seznam.cz*

Škácha P, Sejkora J, Čejka J (2019) Molecular structure of tangdanite from the Jánská vein, Příbram (Czech Republic) - a vibrational spectroscopy study. Bull Mineral Petrolog 27(1): 205-211 ISSN 2570-7337

Abstract

We have undertaken a study of the copper arsenate sulphate mineral tangdanite from the Jánská vein, Příbram, central Bohemia (Czech Republic). Tangdanite has been found on a few specimens and forms individual radial aggregates up to 3 mm in size composed of platy crystals with perfect cleavage. Tangdanite aggregates usually grow on chrysocolla, or more rarely on hematitized rock. The quantitative chemical analyses of tangdanite agrees well with the proposed ideal composition and corresponds to the following empirical formula: $Ca_{1.96}Cu_{9.01}Zn_{0.02}(AsO_4)_{4.06}(PO_4)_{0.01}(SO_4)_{0.51}(OH)_{8.76}\cdot 9H_2O$ (on the basis of 11 cations *pfu*). Tangdanite is monoclinic, space group *C2/c*, with unit-cell parameters: *a* 54.3218(8), *b* 5.5685, *c* 10.469 Å, β 96.294°, *V* 3147.7 Å^3; due to strong preferred orientation on sample, only *a* parameter was refined. Raman bands at 3486, 3046 and 2907 cm^{-1} and infrared bands at 3475, 3310 and 3015 cm^{-1} are assigned to the ν OH stretching of structurally distinct differently hydrogen bonded water molecules and hydroxyls. A Raman band at 1621 cm^{-1} and infrared bands at 1662 and 1611, 1601 cm^{-1} are assigned to the ν_2 (δ) H_2O bending vibrations of structurally distinct hydrogen bonded water molecules. Infrared bands at 1120, 1083, 1065 and 1027 cm^{-1} are assigned to the ν_3 $(SO_4)^{2-}$ antisymmetric stretching and the ν_1 $(SO_4)^{2-}$ symmetric stretching vibrations. Raman band at 997 cm^{-1} and infrared band at 981 cm^{-1} are connected with the ν_1 $(SO_4)^{2-}$ symmetric stretching vibration. Infrared band at 946 cm^{-1} may be connected with (to) the δ M-OH bending vibration. A dominant Raman band at 850 cm^{-1} is attributed to (with) the ν_1 $(AsO_4)^{3-}$ symmetric and a Raman band at 801 cm^{-1} and an infrared band at 791 cm^{-1} to (with) the ν_3 $(AsO_4)^{3-}$ antisymmetric stretching vibrations. Infrared bands at 668 and 610 cm^{-1} may be connected to libration modes of water molecules and to the ν_4 (δ) $(SO_4)^{2-}$ bending vibrations. A Raman band at 509 cm^{-1} and an infrared band at 543 cm^{-1} are assigned to the ν_4 (δ) $(SO_4)^{2-}$ triply degenerate bending vibrations, Raman bands at 467 and 415 cm^{-1} and infrared bands and shoulders at 481, 465 and 422 cm^{-1} are connected with the ν_2 (δ) $(SO_4)^{2-}$ bending and to the ν_4 (δ) $(AsO_4)^{3-}$ bending vibrations. Raman bands at 382, 366 and 314 cm^{-1} may be related to the ν_2 (δ) $(AsO_4)^{3-}$ bending vibrations. A Raman band at 268 cm^{-1} may be assigned to the ν (O-H×××O) stretching vibration. Raman bands at 171, 154, 127, 92 and 55 cm^{-1} are assigned to lattice modes. Raman and infrared spectroscopy confirms absence of $(CO_3)^{2-}$ groups in the crystal structure of studied tangdanite.

Key words: *tangdanite, unit-cell parameters, chemical composition, Raman spectroscopy, infrared spectroscopy, Jánská vein, Příbram, Czech Republic*

Obdrženo 5. 5. 2019; přijato 8. 7. 2019

Introduction

The story of tyrolite-like minerals is interesting and a little bit complicated. Mineral tyrolite was first described by A. G. Werner in 1817 (published in Haidinger 1845) from the locality Schwaz-Brixlegg, Tyrol (Austria). Church (1895) proposed to tyrolite the formula $CaCu_5(AsO_4)_2(CO_3)(OH)_4\cdot 6H_2O$ on the basis of wet chemical analysis. Berry (1948) described tyrolite as orthorhombic, probable space group *Pmma,* with carbonate lacking formula $Cu_9Ca_2(AsO_4)_4(OH)_{10}\cdot 10H_2O$. Palache et al. (1951) considered the formula of tyrolite to be uncertain with respect to the presence of carbonate and/or sulphate. Guillemin (1956) reported the formula $CaCu_5(AsO_4)_2(CO_3)(OH)_4\cdot 6H_2O$ to tyrolite and considered orthorhombic symmetry and space group *Pmma.* Li et al. (2004) reported 0.75 wt. % SO_3 in tyrolite from China. Ma et al. (1980) published a new tyrolite-like mineral named *clinotyrolite* with the formula $Cu_9Ca_2[(As,S)O_4)]_4(OH,O)_{10}\cdot 10H_2O$ and monoclinic symmetry with space group *Pa* or *P2/a,* and pointed out that it is a monoclinic polymorph of tyrolite. Krivovichev et al. (2006) studied two samples of tyrolite from the type locality (Brixlegg, Schwaz, Austria) and found their monoclinic symmetry and determined crystal structure of two polytypes (-1*M* and -2*M*). On the basis of crystal structure study and not reported Raman spectra (presence of carbonate and lacking of sulphates) Krivovichev et al. (2006) proposed formula $Ca_2Cu_9(AsO_4)_4(CO_3)(OH)_8(H_2O)_{11}\cdot nH_2O$ where n = 0 - 1. Števko et al. (2011) studied tyrolite from the Farbiště (Slovakia) and found its two different types - the first (emerald to grass green) with increased SO_4 contents in the range 0.20 - 0.30 *pfu* and relatively low calculated contents of carbonate group (0.08 - 0.17 *pfu*). The second (pale blue-green) type contains significantly less SO_4 (0.04 - 0.09 *pfu*) and calculated contents of carbonates varying in the range 0.31 - 0.64 *pfu*. The differences in composition of those two

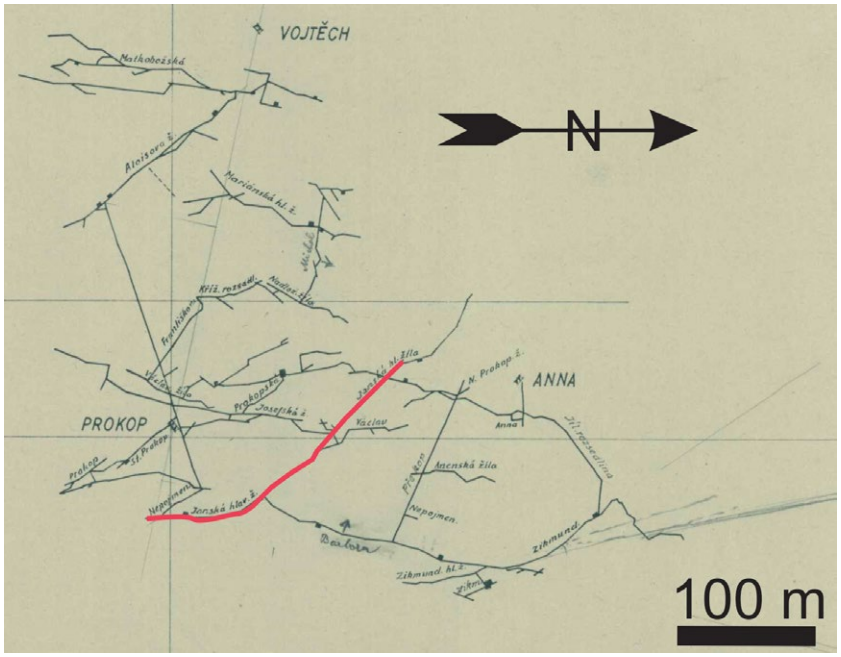

Fig. 1 *Mining situation on the 3rd level of the central part of the Březové Hory deposit; the Jánská vein is marked by red colour.*

Fig. 2 *Rich aggregate of tangdanite from the Jánská vein with perfect cleavage; field of view 4 mm; photo P. Škácha.*

Fig. 3 *Tangdanite crystal aggregate from the Jánská vein; field of view 4 mm; photo P. Škácha.*

types were also confirmed by infrared absorption spectra. Later, Ma et al. (2014) described from Tangdan and Nanniping mines (Yunnan, China) a new mineral phase tangdanite with ideal composition $Ca_2Cu_9(AsO_4)_4(SO_4)_{0.5}(OH)_9 \cdot 9H_2O$, monoclinic symmetry and space group *C2/c*, which corresponds to (SO_4)-dominant analogue of tyrolite without carbonate groups.

Although the description of tangdanite and refinement of its crystal structure have been published recently (Ma et al. 2014), Raman spectroscopic studies of well-defined samples have not been undertaken so far. Moreover, Raman spectroscopy has been proven as an excellent technique for the study of molecular structure of minerals containing complex oxyanions (e.g., Jirásek et al. 2017; Mikuš et al. 2017; Dufresne et al. 2018; Sejkora et al. 2019; Pauliš et al. 2019). Therefore, we have undertaken a vibration spectroscopy study of tangdanite, found at the Jánská vein, Příbram (Czech Republic). This paper aims to summarize results of the complex mineralogical study of this copper calcium arsenate sulphate mineral.

Occurrence and specimen description

Tangdanite was found on samples from the Jánská vein at 3rd level of the Prokop mine (Fig. 1). The Jánská vein is one of less important veins in the Variscan base-metal Březové Hory ore deposit in the central part of the Březové Hory ore district. It was exploited from 13th century till 1978 for Ag, Pb, Zn and Sb ores. Small occurrences of uraninite were occasionally mined there a few years after World War II, especially from the Prokop and Lill mines. About 1 ton of U was recovered from the Jánská vein ores (Škácha et al. 2009). A rich association of supergene and primary mineralization was described from the Jánská vein so far (Plášil et al. 2010a,b, 2014; Sejkora et al. 2003; Škácha et al. 2009).

The surrounding rocks of the Jánská vein are Lower Cambrian greywackes, sandstones and conglomerates. Dolerite dikes often in-

trude sedimentary rocks and the ore veins usually follow them along the same tectonic structures. The ores on the Jánská vein were mined from surface down to the 18th level. Two main ore pillars were found at the Jánská vein (Škácha et al. 2009). The northern ore pillar, which is located near the Jánská shaft, is vertical, splays out to the depth and its position is probably controlled by the Václav vein and the Clay Fault. The southern ore pillar, localized in the southeastern part of the Jánská vein, where mining was concentrated during the period 1948 - 1949, was dipping ca. 35° to the southeast (in a vertical projection of the Jánská vein). Joint occurrence of uranium and copper mineralization without any occurrences of macroscopic galena (in the area of 1st and 2nd level) is typical. Tangdanite occurrence probably comes from the southern ore pillar according to its content of copper mineralization. Its origin is probably bound with Quarternary weathering of primary Cu-mineralization (tennantite) in conditions of oxidation zone *in-situ*.

Tangdanite has been found on a few specimens and forms individual radial aggregates up to 3 mm in size composed of platy crystals with perfect cleavage (Fig. 2, 3). Tangdanite aggregates usually grow on chrysocolla or more rarely on hematitized rock. Its colour is blue-green to emerald green. The associated blue chrysocolla forms crusts up to 2 mm thick with globular glossy aggregates up to 1 mm in the cavities.

Chemical composition and X-ray powder diffraction

Samples of tangdanite were analysed with a Cameca SX-100 electron microprobe (Masaryk University, Brno) operating in the wavelength-dispersive mode with an accelerating voltage of 15 kV, a specimen current of 10 nA, and a beam diameter of 5 μm. The following lines and standards were used: *K*α: andradite (Ca), baryte (S), lammerite (Cu), fluorapatite (P), ZnO (Zn); *L*α: lammerite (As). Peak counting times (CT) were 20 s for main elements and 60 s for minor elements; CT for each background was one-half of the peak time. The raw intensities were converted to the concentrations automatically the using *PAP* (Pouchou, Pichoir 1985) matrix-correction software. The elements Al, Bi, Cl, Co, F, Fe, K, Mg, Na, Ni, Pb, Si and Sb were sought, but found to be below the detection limit (about 0.05 - 0.10 wt. %). Water content could not be analysed directly because of the minute amount of material available. The H_2O content was confirmed by Raman and infrared spectroscopy and calculated from stoichiometry of ideal formula.

Chemical composition of tangdanite sample (Tab. 1) agrees very well with the ideal formula of tangdanite $Ca_2Cu_9(AsO_4)_4(SO_4)_{0.5}(OH)_9 \cdot 9H_2O$, proposed by Ma et al. (2014). The cationic sites are occupied by Ca and Cu with only minor contents of Zn (up to 0.03 *apfu*). The tetra-

Table 1 *Chemical composition of tangdanite (wt. %)*

	Příbram (this paper)			Ma et al. (2014)	Li et al. (2004)	Ma et al. (1980)	Števko et al. (2011)[1]
	mean	range					
CaO	7.06	6.94	- 7.20	7.29	7.13	7.24	7.01
CuO	46.04	45.49	- 47.00	45.71	44.58	46.04	44.91
ZnO	0.13	0.08	- 0.17				0.16
As_2O_5	29.96	29.79	- 30.15	29.82	30.91	28.09	29.99
P_2O_5	0.07	0.06	- 0.07				0.43
SO_3	2.61	2.42	- 2.77	1.60	0.75	1.28	1.32
H_2O*	15.48			15.58	16.63	17.63	17.98
total	101.34			100.00	100.00	100.28	102.27

Mean and range of 3 point analyses; H_2O* contents were calculated on the basis of charge balance and 9 H_2O molecules in ideal formula; [1] - Števko et al. (2011) determined in sample of emerald green "*tyrolite*" from Farbiště also PbO 0.07, F 0.12 and calculated content of CO_2 0.33 wt. %.

Table 2 *X-ray powder diffraction data of tangdanite from Příbram*

h	*k*	*l*	d_{obs}	I_{obs}	d_{calc}	*h*	*k*	*l*	d_{obs}	I_{obs}	d_{calc}	*h*	*k*	*l*	d_{obs}	I_{obs}	d_{calc}
2	0	0	26.99	100.00	27.00	14	0	0	3.857	0.44	3.857	28	0	0	1.9284	0.12	1.9284
4	0	0	13.50	36.00	13.50	16	0	0	3.375	1.38	3.375	30	0	0	1.7999	0.03	1.7998
6	0	0	8.999	0.39	8.999	20	0	0	2.700	0.85	2.700	32	0	0	1.6874	0.09	1.6873
8	0	0	6.746	0.12	6.749	22	0	0	2.4543	1.61	2.4543	34	0	0	1.5881	0.07	1.5881
10	0	0	5.400	0.47	5.399	26	0	0	2.0767	0.40	2.0767	36	0	0	1.4998	0.08	1.4998
12	0	0	4.500	0.49	4.500												

Table 3 *Unit-cell parameters for tangdanite (for monoclinic space group C2/c)*

		a [Å]	*b* [Å]	*c* [Å]	*β* [°]	*V* [Å^3]
Příbram	this paper	54.3218(8)	5.5685*	10.469*	96.294*	3147.7*
Dongchuan[1]	Ma et al. (2014)	54.490(9)	5.5685(9)	10.469(2)	96.294(3)	3157.4(9)
Dongchuan[2]	Ma et al. (2014)	54.443(8)	5.575(1)	10.475(2)	96.24(1)	3161(5)

* due to strong preferred orientation only *a* parameter was refined; [1] - single crystal data; [2] - X-ray powder data

hedral sites are dominated by As and only partly substituted by P (0.01 - 0.02 *apfu*). The determined contents of $(SO_4)^{2-}$ in the interlayer in the range 0.48 - 0.53 *pfu* indicate absence of carbonate ions in this space, which is confirmed by vibrational spectroscopy (see below). The empirical formula of tangdanite (mean of 3 analyses) on the basis of 11 cations *pfu* is $Ca_{1.96}Cu_{9.01}Zn_{0.02}(AsO_4)_{4.06}(PO_4)_{0.01}(SO_4)_{0.51}(OH)_{8.76}\cdot 9H_2O$. In comparison with the type material (Ma et al. 2014), tagdanite from Příbram has, in fact, (SO_4) end-member composition. Published analyses (Tab. 1) suggest an existence of possible solid solution between tangdanite and tyrolite.

Powder X-ray diffraction data were collected on a Bruker D8 Advance diffractometer (National Museum, Prague) with a solid-state 1D LynxEye detector using CuK_α radiation and operating at 40 kV and 40 mA. The powder pattern was collected using Bragg–Brentano geometry in the range 2.5 - 60° 2θ, in 0.01° steps with a counting time of 20 s per step. Positions and intensities of reflections were found and refined using the PearsonVII profile-shape function with the ZDS program package (Ondruš 1993) and the unit-cell parameter waw refined by the least-squares algorithm implemented by Burnham (1962). The experimental powder pattern was indexed in line with the calculated values of intensities obtained from the crystal structure of tangdanite (Ma et al. 2014), based on Lazy Pulverix program (Yvon et al. 1977).

The experimental powder data set given in Table 2 significantly differs from the X-ray pattern calculated from the single-crystal data for tangdanite and published data from this mineral from Dongchuan copper mining district (Ma et al. 2014). It is caused by the strong preferred orientation effects due to small amount of material available for the study. The diffraction maxima with indexes of *h00* type were observed only, it is therefore possible to refine only *a* parameter of unit-cell of studied mineral (Tab. 3).

Raman and infrared spectroscopy

The Raman spectra of studied sample were collected in the range 4000 - 30 cm^{-1} using a DXR dispersive Raman Spectrometer (Thermo Scientific) mounted on a confocal Olympus microscope. The Raman signal was excited by an unpolarised red 633 nm He-Ne gas laser and detected by a CCD detector. The experimental parameters were: 100x objective, 40 s exposure time, 100 exposures, 50 μm pinhole spectrograph aperture and 3 mW laser power level. The spectra were repeatedly acquired from different grains in order to obtain a representative spectrum with the best signal-to-noise ratio. The eventual thermal damage of the measured point was excluded by visual inspection of excited surface after measurement, by observation of possible decay of spectral features in the start of excitation and checking for thermal downshift of Raman lines. The instrument was set up by a software-controlled calibration procedure using multiple neon emission lines (wavelength calibration), multiple polystyrene Raman bands (laser-frequency calibration) and standardized white-light sources (intensity calibration).

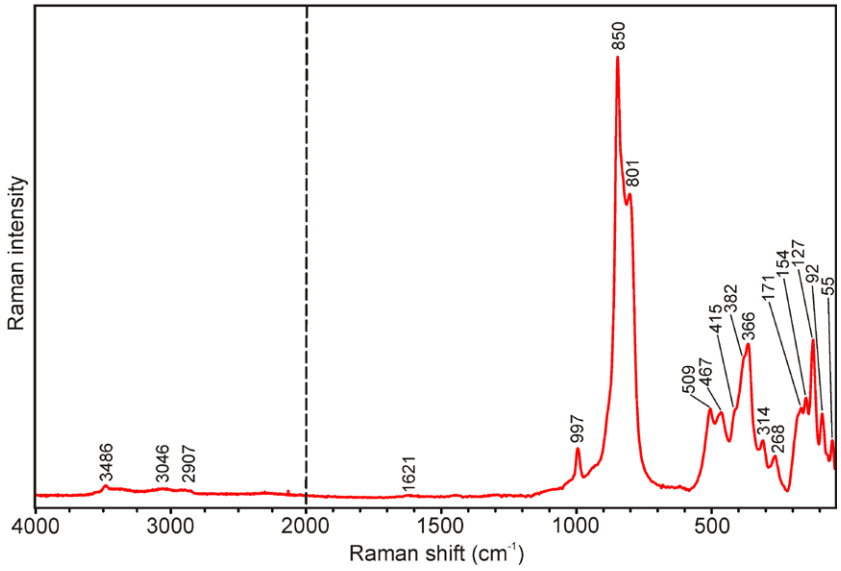

Fig. 4 *Raman spectrum for tangdanite from Příbram (split at 2000 cm^{-1}).*

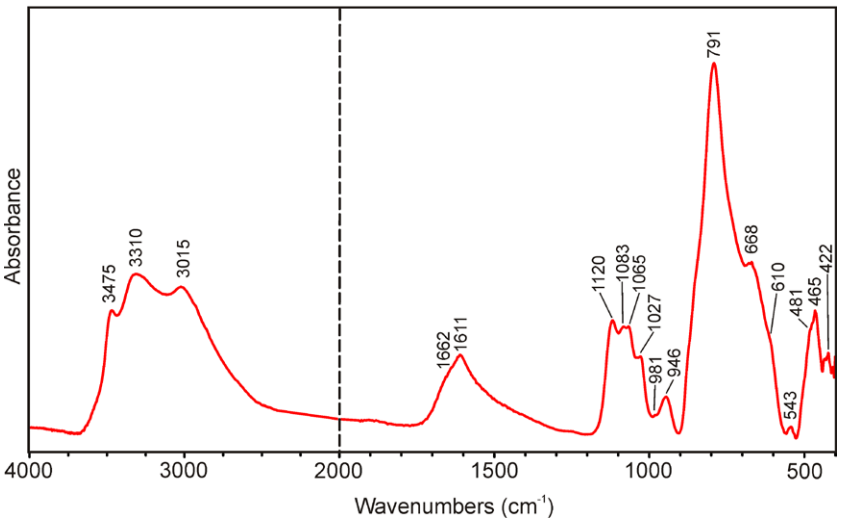

Fig. 5 *Infrared spectrum for tangdanite from Příbram (split at 2000 cm^{-1}).*

The infrared vibrational spectrum of tangdanite was recorded by the attenuated total reflection (ATR) method with a diamond cell on a Nicolet iS5 spectrometer. Spectra over the 4000 - 400 cm^{-1} range were obtained by the co-addition of 64 scas with a resolution 4 cm^{-1} and a mirror velocity of 0.4747 cm/s. Spectra were co-added to improve the signal-to-noise ratio.

In the asymmetric part of the monoclinic (space group *C*2/*c* - C^6_{2h}, *Z* = 4) tangdanite unit cell (Ma et al. 2014), there are symmetrically distinct 1 Ca^{2+} in $Ca(O,H_2O)_6$ octahedra, 5 Cu^{2+} in $Cu(O,OH,H_2O)_6$ octahedra, 2 As^{5+} in $(AsO_4)^{3-}$ tetrahedra, 1 S^{6+} in $(SO_4)^{2-}$ tetrahedra together in interlayer with water molecules and hydroxyls, OH^- (Ma et al. 2014). Infrared spectrum of tangdanite was published and partly intepreted by Ma et al. (2014), who observed following infrared bands 3470, 3340, 3000,

1640, 1604, 1121, 1080, 1029, 940, 850, 810, 671, 475 and 402 cm^{-1}. Frost et al. (2015) described Raman and infrared spectra of tangdanite but their infrared spectrum differs from the spectrum published by Ma et al. (2014) and also from the one presented in this study. The Raman spectrum of Frost et al. (2015) also does not correspond to the Raman spectrum described and interpreted in our study. It is therefore presumable that samples studied by Frost et al. (2015) may not correspond to tangdanite, these authors also did not present any other data (PXRD, EPMA etc.) of these samples. Frost et al. (2015) also state a presence of hydrogenarsenate units in tangdanite but results of the crystal structure study (Ma et al. 2014) do not confirm this assumption.

In free $(AsO_4)^{3-}$ and $(SO_4)^{2-}$ tetrahedra (*T*d symmetry), there are nine normal vibrations, characterized by four fundamental modes of vibrations - ν_1 (A_1) symmetric stretching vibration, Raman active, ν_2 (δ) (E) doubly degenerate bending vibration, Raman active, ν_3 (F_2) triply degenerate antisymmetric stretching vibration, Raman and infrared active, and ν_4 (δ) (F_2) triply degenerate beding vibration, Raman and infrared active. Nakamoto (2009) assigned to tetrahedral $(AsO_4)^{3-}$ and $(SO_4)^{2-}$ vibrations following wavenumbers: $(AsO_4)^{3-}$ 837, 349, 878 and 463 cm^{-1}, respectively, and $(SO_4)^{2-}$ 983, 450, 1105 and 611 cm^{-1}, respectively. Symmetry lowering *T*d → C_{3v}, C_{2v}, C_1 may be connected with infrared activation of infrared inactive vibrations and splitting of degenerate vibrations. For the classification of molecular vibrations, the total reducible representation decomposes into $\Gamma = A_1 + E + 2F_2$ vibrations (Mielke, Ratajczak 1972; Vansant et al. 1973). According to Nakamoto (2009), the octahedra XY_6 are generally characterized by six normal modes of vibrations, of which three are Raman active (ν_1, ν_2 and ν_5), two infrared active (ν_3 and ν_4), and one is inactive in infrared and Raman spectrum (ν_6). This relates from the general point of view to $Ca^{2+}(O,H_2O)$ and $Cu^{2+}(O,OH,H_2O)$ octahedra.

The full-range Raman and infrared spectra of tangdanite from Příbram are given in Figs. 4 and 5, tabulated values in Table 4. Weak Raman bands at 3486, 3046 and 2907 cm^{-1} and strong infrared bands at 3475, 3310 and 3015 cm^{-1} are assigned to the ν OH of differently strong hydrogen bonded water molecules and hydroxyl ions. According to Libowitzky (1999), O-H×××O hydrogen bond lengths vary approximately from 2.88 to 2.64 Å. A very weak Raman band at 1621 cm^{-1} and infrared bands at 1662 and 1611 cm^{-1} are attributed to the ν_2 (δ) H_2O bending vibrations of differently strong hydrogen bonded water molecules.

Table 4 *Tentative interpretation of Raman and infrared spectra for tangdanite*

Raman	infrared	tentative assignment
3486	3475	
3046	3310	ν OH stretch of hydrogen bonded water molecules and hydroxyls
2907	3015	
	1662	ν_2 (δ) bend of hydrogen bonded water molecules
1621	1611	
	1120	
	1083	ν_3 $(SO_4)^{2-}$ antisymmetric and ν_1 $(SO_4)^{2-}$ symmetric stretch
	1065	
	1027	
997	981	ν_1 $(SO_4)^{2-}$ symmetric stretch
	946	δ M-OH bend
850		ν_1 $(AsO_4)^{3-}$ symmetric stretch
801	791	ν_3 $(AsO_4)^{3-}$ antisymmetric stretch
	668	ν_4 (δ) $(SO_4)^{2-}$ bend and molecular water libration modes
	610	
509	543	ν_4 (δ) $(SO_4)^{2-}$ bend
	481	
467	465	ν_2 (δ) $(SO_4)^{2-}$ bend, ν_4 (δ) $(AsO_4)^{3-}$ bend
415	422	
382		
366		ν_2 (δ) $(AsO_4)^{3-}$ bend
314		
268		ν (OH×××O) stretch
171		
154		
127		lattice vibrations
92		
55		

Infrared bands at 1120, 1083, 1065 and 1027 cm^{-1} are assigned to the split triply degenerate ν_3 $(SO_4)^{2-}$ antisymmetric stretching vibrations and the ν_1 $(SO_4)^{2-}$ symmetric stretching vibration, respectively. A coincidence – an overlap with δ M-OH - cannot be excluded. Raman band at 997 cm^{-1} and infrared band at 981 cm^{-1} are connected with the ν_1 $(SO_4)^{2-}$ symmetric stretching vibration. An infrared band at 946 cm^{-1} may be assigned to the δ M-OH bending vibration. A dominant Raman band at 850 cm^{-1} is connected with the ν_1 $(AsO_4)^{3-}$ symmetric and a Raman band at 801 cm^{-1} and an infrared band at 791 cm^{-1} with the triply degenerate ν_3 $(AsO_4)^{3-}$ antisymmetric stretching vibrations. Infrared bands at 668 and 610 cm^{-1} may be attributed to libration modes of water molecules and to the ν_4 (δ) $(SO_4)^{2-}$ triply degenerate bending vibrations. A Raman band at 509 cm^{-1} and an infrared band at 543 cm^{-1} are also assigned to the ν_4 (δ) $(SO_4)^{2-}$ triply degenerate bending vibrations, Raman bands at 467 and 415 cm^{-1} and infrared bands and shoulders at 481, 465 and 422 cm^{-1} are connected with the ν_2 (δ) $(SO_4)^{2-}$ doubly degenerate bending vibrations and to the ν_4 (δ) $(AsO_4)^{3-}$ triply degenerate bending vibrations. Raman bands at 382, 366 and 314 cm^{-1} may be related to the ν_2 (δ) $(AsO_4)^{3-}$ doubly degenerate bending vibrations. A Raman band at 268 cm^{-1} may be assigned to the ν (O-H×××O) stretching vibration. Raman bands at 171, 154, 127, 92 and 55 cm^{-1} are assigned to lattice modes. Some of the Raman bands observed in area from approximately 500 to 200 cm^{-1} may be connected with stretching and bending vibrations of $(Ca,Cu)(O,OH,H_2O)$ octahedra. A coincidence - an overlap of Raman bands - may be therefore expected. Neither Raman nor infrared bands related to $(AsO_3OH)^{2-}$ and/or $(CO_3)^{2-}$ units were observed in the studied tangdanite sample.

Discussion and conclusion

Tangdanite is a supergene mineral formed during the Quarternary weathering of tennantite in conditions of oxidatin zone *in-situ*. Timing of supergene processes in area of the Jánská vein was studied by dating of uranium supergene minerals from the northern part of the Jánská vein (2nd level) (Jarka 2011). Except a few (sub)recently formed minerals (widenmannite, beudantite) there was determined origin of uranium supergene minerals in a wide range between 328.6 ± 107.3 ka (kasolite) and 6.2 ±0,9 ka (metalodévite). Tangdanite probably also origined in this period.

Molecular structure of the well-defined sample of tagdanite from Jánská vein at Příbram can be better constrained using the vibrational spectroscopy. Raman and infrared spectroscopy shows the presence of both $(AsO_4)^{3-}$ and $(SO_4)^{2-}$ units and absence of $(CO_3)^{2-}$ group in the crystal structure of tangdanite. Multiple bands connected with vibrations of water molecules suggest that water is involved in different coordination environments in the structure of tangdanite due to differing hydrogen bond strengths.

Acknowledgements

The authors wish to express their thanks to Radek Škoda (Masaryk University, Brno) for kind support in this study. This work was financially supported by Czech Science Foundation (project GACR 17-09161S).

References

Berry LG (1948) Tyrolite, higginsite, and cornwallite. Am Mineral 33:193

Burnham Ch W (1962) Lattice constant refinement. Carnegie Inst Washington Year Book 61: 132-135

Church AH (1895) A chemical study of some native arsenates and phosphates. Mineral Mag 11: 1-12

Dufresne WJ, Rufledt CJ, Marshall CP (2018) Raman spectroscopy of the eight natural carbonate minerals of calcite structure. J Raman Spectrosc 49(12): 1999-2007

Frost RL, Scholz R. López A (2015) Raman and infrared spectroscopic characterization of the arsenate-bearing mineral tangdanite – and in comparison with the discredited mineral clinotyrolite. J Raman Spectrosc 46: 920-926

Guillemin C (1956) Contribution à la minéralogie des arsenates, phosphates et vanadates de cuivre. Bull Soc Fr Mineral Crist 79*:* 7-95

Haidinger W (1845) Handbuch der bestimmenden Mineralogie. Wien

Jarka P (2011) The dating of the minerals of uranium-polymetallic mineralization of the Jánská vein, Příbram-Březové Hory, ČR, using alpha-spectrometric determination of the radioactive disequilibrium of isotope pairs of uranium decay series. Unpublished MSc. Thesis. Charles University. Prague. 52 pp

Jirásek J, Čejka J, Vrtiška L, Matýsek D, Ruan X, Frost LR (2017) Molecular structure of the phosphate mineral koninckite - a vibrational spectroscopic study. J Geosci 62: 271-279

Krivovichev SV, Chernyshov DY, Döblin N, Armbruster T, Kahlenberg V, Kaindl R, Ferraris G, Tessadri R, Kaltenhauser G (2006) Crystal chemistry and polytypism of tyrolite. Am Mineral 91: 1378-1384

Li Yi, Lai Lairen, Zhou Weining, Qin Chaoke (2004) Mineralogical characteristics and geological significance of tyrolite. Acta Miner Sinica 24: 378-380

Libowitzky E (1999) Correlation of O-H stretching frequencies and O-H×××O hydrogen bond lengths in minerals. Monat Chem 130: 1047-1059

Ma Zhesheng, Li Guowu, Chukanov NV, Poirier G, Shi Necheng (2014) Tangdanite, a new mineral species form the Yunnan Province, China and the discreditation of "clinotyrolite". Mineral Mag 78(3): 559-569

Ma Zhesheng, Qian Rongyao, Peng Zhizhong (1980) Clinotyrolite: a new mineral of hydrous copper arsenate discovered in Dongchuan, Yunnan. Acta Geol Sinica 54: 134-143

Mielke Z, Ratajczak H (1972) The force constants and vibrational frequencies of orthoarsenates. Bulletin de l´Academie Polonaise des Sciences, Série des Sciences Chimiques 20: 265-270

Mikuš T, Patúš M, Luptáková J, Bancík T, Biroň A (2017) Mineralogical characteristics of the secondary calcium carbonates from the Špania Dolina - The first occurrence of monohydrocalcite in ore deposits in Slovakia. Bull Mineral Petrolog 25(2): 318-326

Nakamoto K (2009) Infrared and Raman spectra of inorganic and coordination compounds Part A Theory and applications in inorganic chemistry. John Wiley and Sons Inc. Hoboken, New Jersey

Ondruš P (1993) ZDS - A computer program for analysis of X-ray powder diffraction patterns. Materials Science Forum: 133-136, 297-300, EPDIC-2. Enchede.

Palache C, Berman H, Frondel C (1951) Dana´s System of Mineralogy, 7th Edition. New York

Pauliš P, Vrtiška L, Fuchs P, Adamovič J, Čejka J, Pour O, Malíková R (2019) Iriginite, chistyakovaite and metazeunerite from the 5. květen adit at Vrchoslav in Krušné hory Mts. (Czech Republic). Bull Mineral Petrolog 27(1): 136-147

Plášil J, Čejka J, Sejkora J, Škácha P, Goliáš V, Jarka P, Laufek F, Jehlička J, Němec I, Strnad L (2010a) Widenmannite, a rare uranyl lead carbonate: occurrence, formation and characterization. Mineral Mag 74: 97-110

Plášil J, Palatinus L, Rohlíček J, Houdková L, Klementová M, Goliáš V, Škácha P (2014) Crystal structure of lead uranyl carbonate mineral widenmannite: Precession electron-diffraction and synchrotron powder-diffraction study. Am Mineral 99: 276-282

Plášil J, Sejkora J, Čejka J, Škácha P, Goliáš V, Ederová J (2010b) Characterization of phosphate-rich metaloděvite from Príbram, Czech Republic. Can Mineral 48: 113-122

Pouchou J, Pichoir F (1985) „PAP“ (φρz) procedure for improved quantitative microanalysis. In: Armstrong JT (ed): Microbeam Analysis: 104-106. San Francisco Press. San Francisco

Sejkora J, Čejka J, Škácha P, Gabašová A, Novotná I (2003) Minerals of the zippeite group from the Jánská vein, Březové Hory, Příbram. Bull Mineral Petrolog 11: 183-189

Sejkora J, Tvrdý J, Čejka J, Vrtiška L, Dolníček Z (2019) Bendadaite from Krásno near Horní Slavkov (Czech Republic), description and Raman spectroscopy. Bull Mineral Petrolog 27(1): 63-71

Škácha P, Goliáš V, Sejkora J, Plášil J, Strnad L, Škoda R, Ježek J (2009) Hydrothermal uranium-base metal mineralization of the Janská vein, Březové Hory, Příbram, Czech Republic: lead isotopes and chemical dating of uraninite. J Geosci 54(1): 1-13

Števko M, Sejkora J, Bačík P (2011) Mineralogy and origin of supergene mineralization at the Farbiště ore occurrence near Poniky, central Slovakia. J Geosci 56: 273-298

Vansant FK, Van Der Veken BJ, Desseyn HO (1973) Vibrational analysis of arsenic and its anions. I. Description of the Raman spectra. J Molec Struct 15: 425-437

Yvon K, Jeitschko W, Parthé E (1977) Lazy Pulverix, a computer program for calculation X-ray and neutron diffraction powder patterns. J Appl Cryst 10: 73-74